Point Mutation of Adenosine Triphosphate–binding Motif Generated Rigor Kinesin That Selectively Blocks Anterograde Lysosome Membrane Transport

Takao Nakata and Nobutaka Hirokawa

Department of Anatomy and Cell Biology, School of Medicine, University of Tokyo, Tokyo 113, Japan

Abstract. In the study of motor proteins, the molecular mechanism of mechanochemical coupling, as well as the cellular role of these proteins, is an important issue. To assess these questions we introduced cDNA of wild-type and site-directed mutant kinesin heavy chains into fibroblasts, and analyzed the behavior of the recombinant proteins and the mechanisms involved in organelle transports. Overexpression of wild-type kinesin significantly promoted elongation of cellular processes. Wild-type kinesin accumulated at the tips of the long processes, whereas the kinesin mutants, which contained either a T93N- or T93I mutation in the ATP-binding motif, tightly bound to microtubules in the center of the cells. These mutant kinesins could bind to microtubules in vitro, but could not dissociate from them even in the presence of ATP, and did not support microtubule motility in vitro, thereby indicating rigor-type mutations. Retrograde transport from the Golgi apparatus to the endoplasmic reticulum, as well as lysosome dispersion, was shown to be a microtubule-dependent, plus-end–directed movement. The latter was selectively blocked in the rigor-mutant cells, although the microtubule minus-end–directed motion of lysosomes was not affected. We found the point mutations that make kinesin motor in strong binding state with microtubules in vitro and showed that this mutant causes a dominant effect that selectively blocks anterograde lysosome membrane transports in vivo.

MOTOR proteins have two unique features that allow them to support various cell movements such as intracellular vesicular transports. One is that they convert chemical energy of ATP hydrolysis into mechanical forces, which is essential to the motor activity. The other is that they know which cargoes to transport where and when in the cell, which is necessary to use the forces effectively in the cellular context. To understand the function of motor proteins, an experimental approach to both features is necessary.

Regarding the latter feature, following the biochemical identification of kinesin, a microtubule (MT)[1] plus-end–directed motor protein (Vale et al., 1985; Brady, 1985), and cytoplasmic dynein, a minus-end–directed motor protein (Paschal and Vallee, 1987; Lye et al., 1987), it is generally believed that these two proteins are responsible for the intracellular vesicular and organelle transports. The situation, however, is not so simple. First, recent identification of numerous new members of motor proteins raised a possibility that kinesin and dynein are not the only motor proteins for the vesicular transports to both directions of MTs (for reviews see Goldstein, 1991; Hirokawa, 1993). Second, although a number of studies on the intracellular localization and subcellular fractionation of kinesin supports its role in vesicular transports (Heason et al., 1992; Hirokawa et al., 1991; Marks et al., 1994; Pfister et al., 1989), there are still arguments about which vesicles kinesin transports, suggesting that these approaches alone may not provide us a conclusive answer. More seriously, MT dependent motility is not always necessary for vesicular transports: constitutive secretion, which is a representative of anterograde vesicular transport, is not MT dependent. In fact, nocodazole treatment does not inhibit this secretion, instead only inhibiting the polarized sorting of the vesicles in epithelial cells (Rivas and Moore, 1989). Although nocodazole and colchicine both have been used to study the MT dependence of membrane transports (Heuser, 1989; Lippincott-Schwartz et al., 1990; Rivas and Moore, 1989; Turner and Tartakoff, 1989), they depolymerize MTs and therefore block the motor-dependent transport and the stational anchoring process, both of which are MT-dependent processes. Moreover, they disrupt the integrity of the organelles such as the Golgi apparatus (Turner and Tartakoff, 1989), which makes it difficult to distinguish further between these MT-dependent processes.

Address all correspondence to N. Hirokawa, Department of Anatomy and Cell Biology, School of Medicine, University of Tokyo, 7-3-1 Hongo, Bunkyo-ku, Tokyo 113, Japan. Tel.: 81-3-3812-2111 ext. 3326. Fax: 81-3-5689-4856.

1. *Abbreviations used in this paper*: BFA, brefeldin A; KHC, kinesin heavy chain; MT, microtubule.

We used a new approach to study both the features of motor proteins in vivo and in vitro by introducing a series of site-directed mutations at the ATP-binding consensus motif of the kinesin heavy chain (KHC). These mutants, as well as wild-type KHC cDNAs, were transfected to fibroblasts. The behavior of the mutated proteins in the cells provided us information on their motor activity. Their biochemical property and in vitro motility assay were also examined using a recombinant protein expressed in insect cells. Their possible role as cytoplasmic motors was evaluated by the ability to interfere in vivo with the intracellular movements. Our approach provides a new method to assess the motor functions of genetic-engineered proteins in vivo and in vitro, and also allows the investigation of membrane trafficking in cells by enabling the perturbation of a specific motor protein function.

Materials and Methods

Antibodies and Reagents

Mouse KHC cDNA was kindly provided by Dr. K. Kato (MRC Molecular Genetics Unit, Cambridge, UK) (Kato, 1991). Mouse mAbs to kinesin (H1 and H2) were gifts from Dr. G. Bloom (University of Texas, Austin, TX) (Pfister et al., 1989), while antibody to β-COP (M3A5) was a gift from Dr. T. Kreis (University of Kyoto, Kyoto, Japan). Rat anti-tubulin antibody (YL1/2) was purchased from BIOSYS S. A. (Compiegne, France). Rat mAb (ABL93) to lysosomal protein (Lamp-2) was obtained from the Developmental Studies Hybridoma Bank maintained by the Department of Pharmacology and Molecular Sciences, Johns Hopkins University School of Medicine (Baltimore, MD), and the Department of Biological Sciences, University of Iowa (Iowa City, IA), under contact No. 1-HD-2-3144 from the National Institute of Child Health and Human Development. Human CD8 expression vector and antibody to CD8 were gifts from Dr. S. Frutani (Department of Immunology, University of Tokyo, Tokyo, Japan). Anti-dynamin antibody and dynamin expression vector were characterized in our previous paper (Noda et al., 1993). Mitotracker and BODIPY-ceramide were purchased from Molecular Probes, Inc. (Eugene, OR). Brefeldin A was purchased from Wako Chemicals (Osaka, Japan) and stocked as 3.5 mM solution in ethanol at −20°C.

Cells and Transfection

Mouse fibroblast L cells were grown in DME supplemented with 10% FCS. All cells were grown at 37°C in a humid atmosphere of 95% air and 5% CO_2. One day before transfection, cells were plated on a poly-L-lysine–coated coverslip. Transfection was performed by the Ca-phosphate method (Chen and Okayama, 1987). All assays were carried out 48 h after transfection.

PCR-mediated Site-directed Mutagenesis

We designed PCR primers to introduce a new restriction site (SpeI) that does not change the translated amino acid sequence within 15 base pairs from the mutation sites. PCR was then performed between the appropriate NH_2-terminal site (BamHI) and mutagenized site, and between the mutagenized site and appropriate COOH-terminal site (ClaI). Primers for PCR around the mutagenized sites were TGAACTAGTCTGCCCATATGCAAAAATTGTTCC (reverse), and CAGACTAGTTCAG(ATC)AAAAACTCATACCATGGAGGGG (forward for G91 mutants) CAGACTAGTTCAGGAAAAA (ATG)TCATACCATGGAGGGGAAG (forward for T93 mutants). The amplified fragments were digested with respective restriction enzymes, and both fragments were ligated into BamHI–ClaI-digested kinesin cDNA. Before sequencing, the transformants were checked by SpeI digestion.

It was easy to find base substitutions for a new restriction site located around a given site that is to be mutagenized. Once a new site is introduced, adding more mutations becomes much easier than before because the ligation of two fragments with cohesive sites is sufficient to produce the mutations by the PCR method. Thus, this technique is considered convenient for introducing systematic mutations around the motifs of biological significance.

Construction of Mammalian Expression Vectors

The Kozak sequence for eukaryotic expression was introduced just before the initial ATG codon of murine KHC cDNA by the PCR method (Navone et al., 1992). Next, full-length cDNAs of authentic and mutant KHCs were ligated into the pHβAPr1-neo vector at the SalI site (Noda et al., 1993).

Baculovirus Expression Study

Wild-type and T93N-mutant KHC cDNA was cut at internal XhoI site (at 2,667 bp) and ligated with the 6-histidine tag sequence with stop codon (CTCGAGACCACCACCACCACCACCACTGA). These KHC cDNAs, which include the head domain and three-fourths of the rod domain, was ligated into the pBacPAK9 (Clontech Laboratories, Inc., Palo Alto, CA) at EcoRI and XbaI sites. Recombinant viruses were obtained by the cotransfection of the plasmid and Bsu36I-digested BacPAK6 virus DNA to *Spodoptera frugiperda* (Sf9) cells. Recombinant baculovirus vectors for T93I- and T93S mutants were also prepared in the same way.

For expression of the KHCs, Sf9 cells were harvested 48 h after infection with the recombinant virus. The cells were lysed in PEM buffer (80 mM Pipes, 2 mM $MgCl_2$, and 2 mM EGTA, pH 7.0) with 0.1% Triton X-100, and centrifuged at 100,000 *g* for 30 min. These supernatants were used for MT-binding assay and nickel-column purification. For the MT-binding assay, the supernatants were incubated for 20 min with one-tenth vol of 5 mg/ml taxol-polymerized MTs in the presence of 2 mM AMP-PNP (5′-adenylyl imidodiphosphate), and centrifuged at 100,000 *g* for 30 min at 37°C. Then the pellets were homogenized in the PEM buffer containing 5 mM Mg ATP by passing through the 23-gauge syringe, incubated for 20 min at 37°C, and again centrifuged. Throughout the experiments, the wild-type KHC and the T93N mutants were dealt with in precisely the same manner, that is, the same number of the cells were infected with the same titer

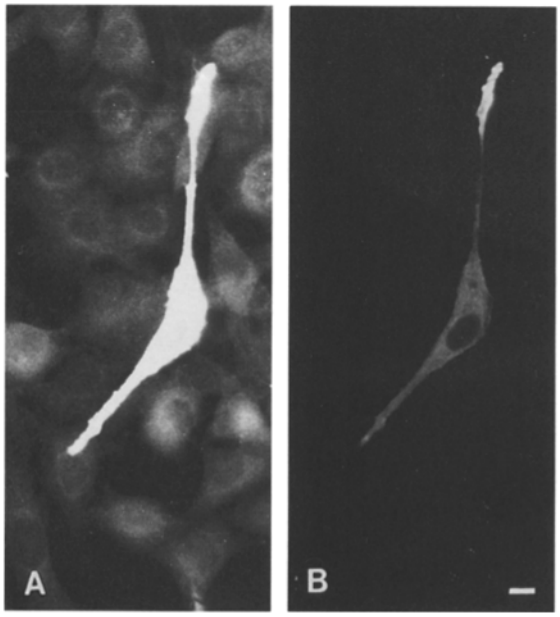

Figure 1. Endogenous and exogenous expression of kinesin in mouse fibroblast cells. L cells were transfected with cDNA of KHC, and stained with H2 antibody 48 h later. The same negative was printed with short exposure time (*A*) and long exposure time (*B*). It is a transient expression system, and only a few percent of cells express the exogenous protein. The brightly stained cell with halos is the transfected cell (*A*). The staining of the surrounding cells shows the localization of endogenous kinesin in L cells (*A*). Note that the transfected cell in *A* is so bright that subcellular distribution of exogenous kinesin cannot be resolved. Bar, 10 μm.

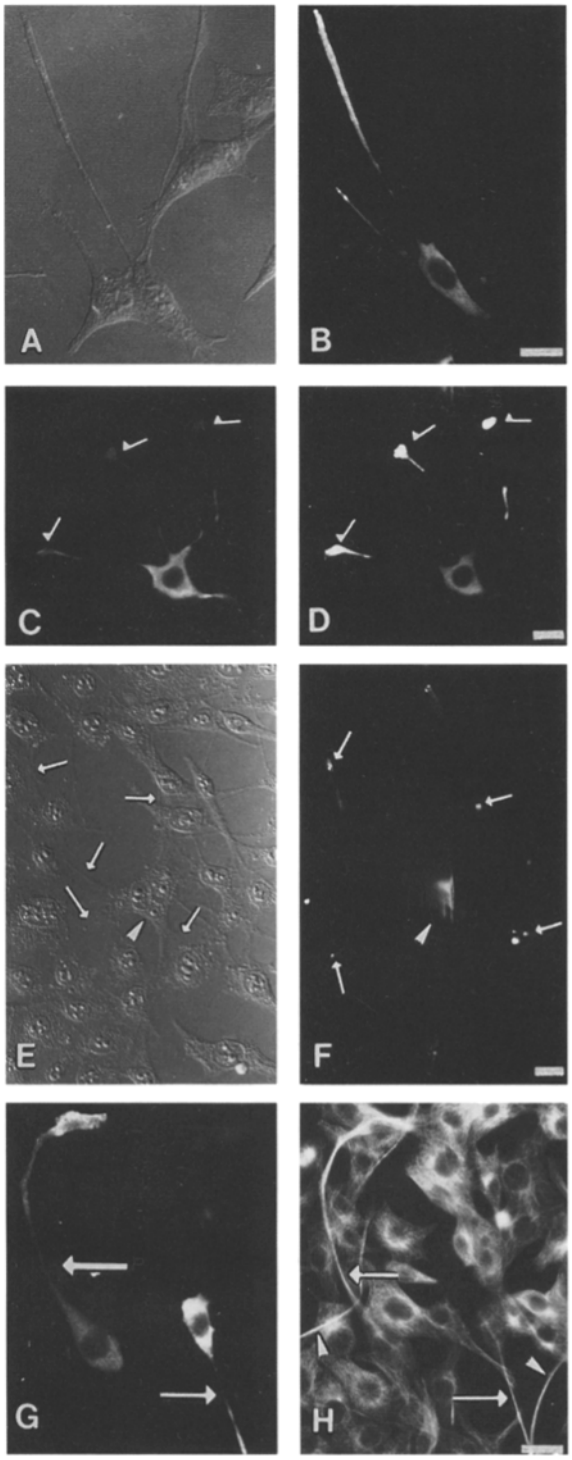

Figure 2. Localization of wild-type kinesin heavy chain in transfected cells. Mouse L cells were transfected with the wild-type kinesin cDNA and analyzed by fluorescence labeling 48 h after transfection. Nomarski image (*A*) and antikinesin staining (*B*) of a transfectant. Kinesin accumulates at the tips of the processes and is diffusely localized in the cell body. (*C* and *D*) Cotransfection of cDNAs of KHC and dynamin GTPase. Cells expressing both proteins were double labeled with anti-dynamin antibody (*C*) and anti-kinesin antibody (*D*). Kinesin accumulates at the tips (*arrows*), whereas dynamin is localized throughout the cytoplasm. (*E* and *F*) Cells were extracted with 0.02% saponin before fixation and stained with anti-kinesin antibody. The transfected cell (*arrowhead*) has several processes (*arrows, E*), though most of the kinesin was extracted from the cell body and processes. Only small dot staining is apparent at the tips (*arrows, F*), being much less than the staining of the tips in nonextracted cells (*B, D,* and *G*). (*G* and *H*) Double labeling of kinesin (*G*) and tubulin (*H*). Long processes of transfectants contain MTs (*arrows*). Note that these processes are also present in nontransfected cells (*arrowheads*). Bars, 20 μm.

of virus, and extracted in the same amount of buffer, and loaded with the same amount of samples on 7.5% SDS-PAGE.

For in vitro motility assay, the cell extracts were purified with 1 ml chelating sepharose column by FPLC system (Pharmacia LKB Biotechnology, Inc., Piscataway, NJ). The recombinant proteins were eluted at 400–500 mM imidazole in the PEM buffer. The peak fractions were collected, and desalted with gel filtration with PD-10 column (Pharmacia LKB Biotechnology, Inc.). These samples were used for in vitro motility assay (Nakata et al., 1993). Briefly, a small chamber was made by attaching a coverslip to a slide glass with tape (Scotch; 3M, St. Paul, MN). Purified motor protein solution was applied to the chamber, and incubated for 5 min. After a wash of the chamber with PEM, taxol-polymerized MTs and 2 mM Mg-ATP were applied. MTs were visualized by (video-enhanced contrast, differential interference contrast) (AVEC-DIC) microscopy.

Immunocytochemistry

For Fig. 1, the cells were fixed with 2% paraformaldehyde-PBS for 15 min at ambient temperature, permeabilized with 0.2% saponin-PBS for 10 min, and blocked with 10% FCS. Then they were incubated with H2 antibody (×100 ascites) at 37°C for 1 h, washed three times with 10% FCS-PBS, and incubated again with FITC-labeled anti–mouse IgG. After extensive wash with PBS, they were mounted in DABCO-PBS. The cells were then examined with an Axiophot (Carl Zeiss, Inc., Thornwood, NY) equipped with Plan-Apochromat 40× objective and photographed with Tri-X 400 (Eastman Kodak Co., Rochester, NY) for 20-s exposure. The negatives were printed with different exposure time longer (Fig. 1 *A*) and shorter (Fig. 1 *B*). For the most of the experiments, the cells were fixed with ice-cold methanol for 1 min, washed with PBS, and blocked with 2% BSA-PBS for 15 min. Next, they were stained with first and second antibodies for the organelle marking, and then stained with a mixture of H1 and H2 antibodies (×100 ascites) for 15 min followed by a 15-min incubation with rhodamine-labeled anti–mouse IgG and FITC-labeled anti–rat IgG. Mitotracker was used per the manufacturer's instructions. The cells were examined and photographed using an Axiophot equipped with MRC1000 confocal microscopy system.

For the saponin extraction, the cells were extracted for 10 min with 0.02% saponin in PEM buffer (100 mM Pipes, pH 6.9, 5 mM $MgCl_2$, 5 mM EGTA) containing 0.5 mM GTP, 1 μM taxol, and 1 mM PMSF and 0.1 mM leupeptin with or without 5 mM ATP at 37°C, then fixed with 2% paraformaldehyde, 0.1% gultaraldehyde-PEM containing taxol and the protease inhibitors for 15 min at ambient temperature (Hirokawa, 1982; Nakata and Hirokawa, 1992). The cells were treated with 0.1% Triton X-100-PBS for 5 min and quenched with 50 mM glycine-PBS for 2 × 5 min. Then the cells were blocked with 2% BSA-PBS for 10 min and stained with anti-kinesin and anti-tubulin antibody.

For quantification of the fluorescence, the wild-type and the mutant cells were prepared at the same time, and processed for immunocytochemistry in the same procedure. The antibodies used (H1 and H2) do not recognize the mutated sites. They were then examined with an Axiophot using ×40 oil-immersed objectives equipped with MRC-1000 confocal system. Data were collected as Z series throughout the cells at 1-μm intervals under the fixed laser and Epi-detector conditions. The maximal Z projection of these images was used for the analysis, because it reflects local density of the fluorescence irrespective of the width of the cells along the Z-axis. All the pixels covered with each transfected cell were integrated, and the average pixel was obtained by dividing the value by the area covered with the cell. This average pixel was used as the indicator of the expression level of the exogenous kinesin in the cells.

Lysosome Assay

Lysosome motility was assayed according to Heuser (1989). Briefly, 48 h after transfection, the cells were removed from the CO_2 incubator and washed three times over 15 min in Ringer's solution (155 mM NaCl, 5 mM KCl, 2 mM $CaCl_2$, 1 mM $MgCl_2$, 2 mM NaH_2PO_4, 10 mM Hepes buffer,

pH 7.2, 10 mM glucose, and 0.5 mg/ml BSA), then incubated for 30 min at 37°C. Cells were again incubated for 15 min in either acetate-Ringer's solution (80 mM NaCl, 70 mM Na-acetate, 5 mM KCl, 2 mM $CaCl_2$, 1 mM $MgCl_2$, 2 mM NaH_2PO_4, 10 mM Hepes buffer, pH 6.9, and 10 mM glucose), or NH_4Cl-Ringer's solution (30 mM NH_4Cl in the above normal bicarbonate-free Ringer's solution). Cells were subsequently fixed with ice-cold methanol and processed for immunocytochemistry. For the rebound experiments, NH_4Cl treatment was followed by washing three times with normal Ringer's solution over 5 min, and before fixation the cells were incubated in the acetate-Ringer solution for an additional 15 min.

Golgi Assay

The cells were incubated with 5 μg/ml brefeldin A (BFA) for 15 min and fixed with ice-cold methanol. For the recovery experiments, cells were incubated with 5 μg/ml BFA for 30 min, washed twice with fresh medium, and before fixation further incubated for 15 min. Then the cells were stained with anti-kinesin and anti-β-COP antibody.

For the BODIPY-ceramide staining, L cells were cotransfected with kinesin and human CD8 cDNAs. After 48 h, CD8 membrane marker was stained by the addition of anti-CD8 antibody to the medium, followed by incubation for 15 min at 37°C, changing the medium twice, and further incubating for 15 min with 50× anti-rat IgG antibody. BODIPY-ceramide was prepared by the protocol by Pagano et al. (1991). The cells were incubated with BODIPY-ceramide in Hepes-buffered MEM for 10 min at 37°C, then washed three times with Hepes-buffered MEM over 15 min at 37°C (Pagano et al., 1991). They were again incubated in the same medium with or without 5 μg/ml BFA, then examined with an Axiophot microscope. The CD8-positive cells were photographed, and their positions were noted down. The same samples were subsequently fixed with ice-cold methanol and stained with H1 and H2 antibodies to check the expression of kinesin mutants.

Results

Overexpression of KHC in Fibroblasts Promotes Elongation of Processes

Under the control of β-actin promoter, we introduced the full-length of cDNA of mouse wild-type KHC into mouse fibroblast L cells, then stained them 48 h later with anti-kinesin antibodies (H1 and H2). Although nontransfected L cells expressed some amount of endogenous kinesin molecules (Fig. 1 *A*; Pfister et al., 1989), the transient transfected cells expressed by far higher amount of exogenous kinesin than the surrounding nontransfected cells (Fig. 1 *A*) and consequently, the transfectants were detected easily by immunocytochemistry. Hereafter, we use the staining and printing conditions in Fig. 1 *B*, because the condition in Fig. 1 *A* could not resolve the subcellular localization of overexpressed KHC. Note the diffuse cytoplasmic staining in the transfected cells (Fig. 1).

Most of the transfected L cells showed long processes with round tips (Fig. 2, *A* and *B*). Although thin processes were sometimes found in normal L cells (*arrowheads*, Fig. 2 *F*), the processes were significantly longer in the transfected cells. This tendency was quantitatively analyzed and examined its relationship with the expression level of KHC (Fig. 3). To this aim, we took serial confocal images of antikinesin-stained cells and obtained the maximal Z projection images. Then we quantified the average pixels within the area covered by the cells, which corresponds to the average density of the fluorescence in the whole cells. Then we plotted each transfected cell by the kinesin expression level and the length of the longest process. As shown in Fig. 3, the elongation of processes was observed independent of the kinesin expression level. The number of the processes per cell was not increased in the transfected cells, and monopolar or bipolar cells were often observed.

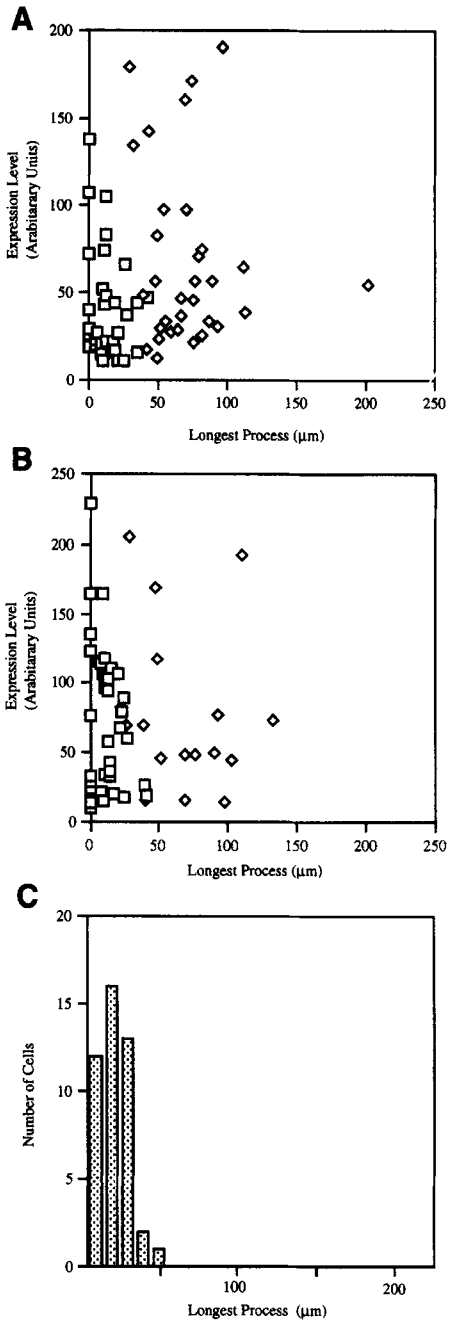

Figure 3. Quantitative analysis of the recombinant KHC expression and cellular process formation. The length of the longest processes of each cells was plotted against the expression level of KHC. *A* and *B* show the results of independent two sets of experiments. *C* shows the control distribution of the nontransfected L cell population. Wild-type, but not rigor-mutant KHC promotes cellular process elongation, almost independent of the protein expression level. *Square*, T93N mutant; *diamond*, wild-type KHC.

Interestingly, the staining with the anti-kinesin antibodies tended to be strongest at the tips, moderate in the cell bodies, and weak in the processes (Figs. 1 *B* and 2 *B*). Accumulation at the tips is known to be specific for kinesin, because cotransfection with dynamin, a nonmotor GTP-

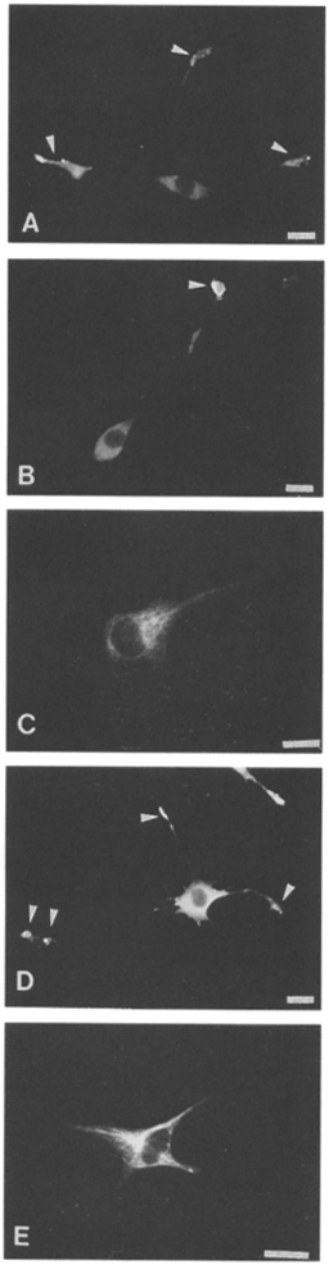

Figure 4. Gallery of mutant KHC-transfected cells. All cells were detected by antikinesin staining: (*A*) G91A, (*B*) G91V, (*C*) T93I, (*D*) T93S, and (*E*) T93N. *A*, *B*, and *D* show similar staining patterns with wild-type kinesin, namely, accumulation at the tips (*arrowheads*) and diffuse cytoplasmic staining. In contrast, *C* and *E* show the strongest staining within the cell bodies. Filamentous staining is also apparent in *C* and *E*. Bars, 20 μm.

binding protein (Noda et al., 1993), showed that although kinesin accumulates at the tips, dynamin instead tends to distribute throughout the cell (Fig. 2, *C* and *D*). One possible explanation for such accumulation is that foreign kinesin's mRNA is preferentially translated at the tips. However, this is considered unlikely, since some mutant kinesins which only have point mutations in their cDNAs, failed to accumulate at the tips (Fig. 4). The staining was reduced markedly when the cells were treated with mild detergent saponin before fixation (Fig. 2, *E* and *F*), and thus we know that this accumulation is not due to the high-affinity binding of the kinesin molecule to the structures in the tips. Although strong, tiny stainings sometimes remained after detergent extraction (*arrows*, Fig. 2 *F*), they were much smaller than the staining of the tips in nonextracted cells (Fig. 2, *B* and *D*). Because they are so intense and sometimes square in shape, we presume they are crystals of kinesin (inclusion bodies).

An alternative possibility is that the expressed kinesin may traverse along the MTs to the tips. Double staining with anti-kinesin and anti-tubulin antibodies showed that these processes contain MTs (Fig. 2, *G* and *H*), and since the MTs have their plus-ends at the cell periphery, anterograde-moving kinesin may travel on the MTs towards the cell periphery. In further support of this hypothesis, mutant kinesins, which are assumed to have severe defects in their motor functions, did not show such localization (Fig. 4), though their rod and tail domains (Yang et al., 1989) remained identical to the wild-type KHC.

Expression of Mutant KHCs in Fibroblasts

Among the kinesin superfamily proteins, two point mutations have been reported to cause a dominant effect on yeast (Meluh and Rose, 1990) and fruit fly cell division (Rasooly et al., 1991). In both cases, an amino acid was substituted at the ATP-binding consensus motif in the motor domain. Based on this knowledge of natural mutants, we designed five new mutant KHC molecules (Table I) which have one amino acid substitution at 91G or 93T. We transfected these mutants into fibroblasts and examined their localization. This was a considerably faster assay to detect the motor defects than the biochemical method after purification of each mutant protein.

These mutant KHCs were classified into two types according to their localization in the transfected cells. The G91A-, G91V-, T93S mutants diffusely localized in the cytoplasm, and especially accumulated at the tips of the long processes (Fig. 4, *A*, *B*, and *D*), having indistinguishable patterns from those of the wild-type KHC. In contrast, the T93N- and T93I mutants showed a somewhat filamentous staining pattern that was most intense in the center of the cells (Fig. 4, *C* and *E*), although long processes were rarely observed (Fig. 3). We focused on T93N mutant, which is a representative of the phenotype quite different from the wild-type kinesin, unless otherwise noted.

T93N- and T93I Mutations Make a Rigor-type Kinesin

Intracellular localization of T93N mutant suggested that this mutation severely impaired the motile property of kinesin, i.e., they tightly bind to, but rarely detach from, MTs. Double labeling with anti-kinesin and anti-tubulin antibodies using permeabilized and nonpermeabilized cells (Fig. 5) shows the colocalization of the mutant kinesins and MTs. With the exception of small tiny dots (Fig. 2 *F*), the wild-type kinesin and G91A-, G91V-, T93S mutants were not detected after permeabilization. On the other hand, the T93N- and T93I mutants remained in the

Table I. Point Mutations of ATP-binding Motifs of KHC

Name	Site of point mutation
Wild-type KHC	GQTSSGKT
G91A mutant	GQTSSAKT
G91V mutant	GQTSSVKT
T93I mutant	GQTSSGKI
T93S mutant	GQTSSGKS
T93N mutant	GQTSSGKN

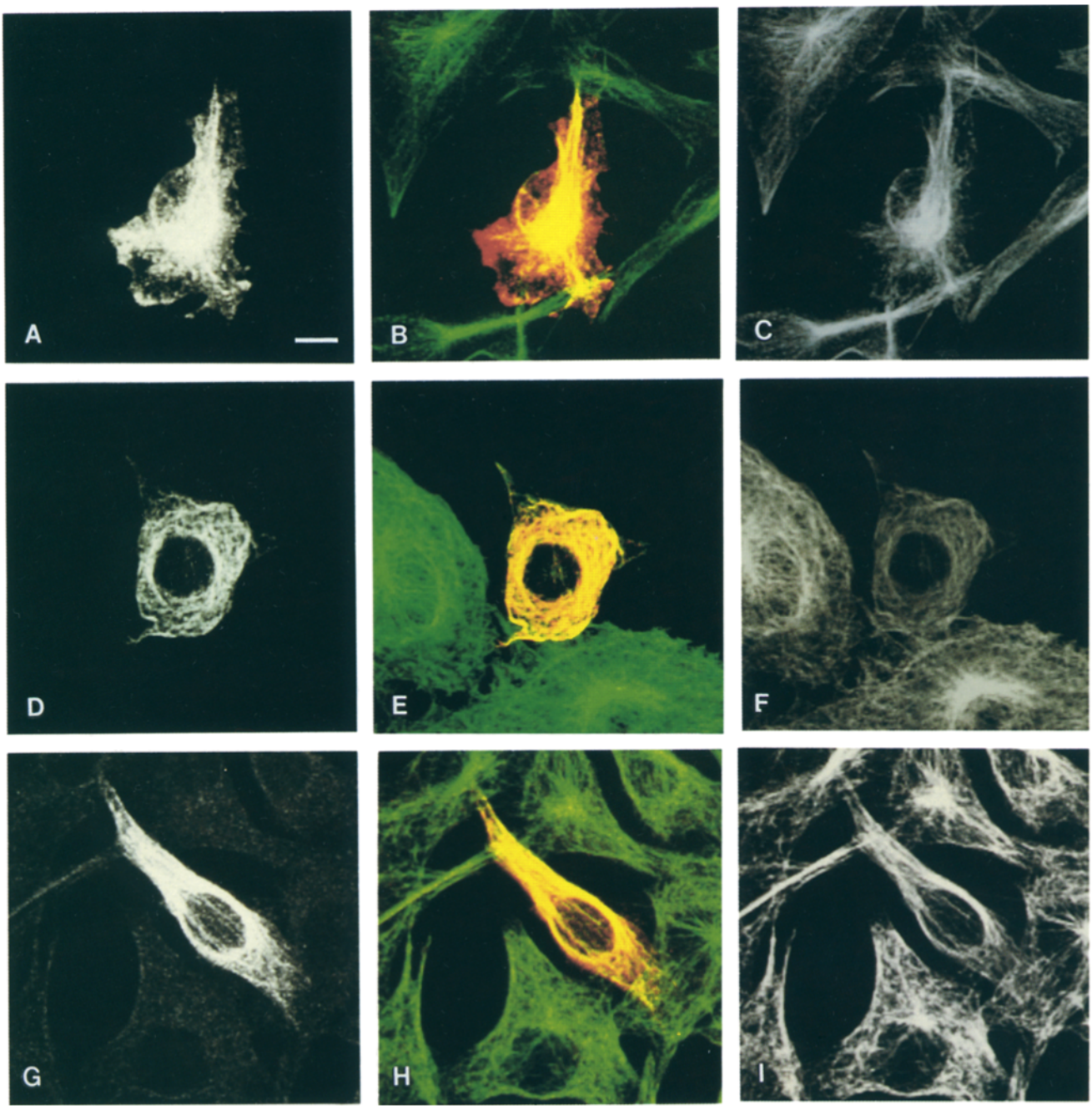

Figure 5. Colocalization of T93N mutant with MTs. Confocal images of double labeling of T93N-transfected cells with anti-kinesin antibody (*A*, *D*, and *G*), and anti-tubulin antibody (*C*, *F*, and *I*). Both stainings are superimposed in *B*, *E*, and *H* using red filter for the kinesin staining and green filter for the MT staining. (*A–C*) Cells were fixed without extraction. Most of KHCs colocalized with MTs (*yellow*, *B*), but some remains in the soluble pool (*red*). (*D–F*) Cells were extracted with 0.02% saponin in the absence of ATP. KHC colocalized with MTs (*yellow*, *E*), but at the edges of cells, MT staining prevailed (*green*). (*G–I*) Cells were extracted with 0.02% saponin in the presence of 5 mM Mg-ATP. KHC still colocalized with MTs. Bar, 10 μm.

cell body after saponin extraction and showed colocalization with MTs even in the presence of 5 mM ATP (Fig. 5), a behavior indicating their strong binding to MTs. This finding suggests that T93N- and T93I-mutant kinesin molecules attach to the nearest MTs, but cannot traverse along them.

To show this property more directly, we transferred these wild-type and T93N-mutant kinesins to baculovirus expression system. For this purpose, we truncated kinesins at the COOH-terminal quarter of the rod domain and added 6 histidine tags. The molecular mass of the recombinant proteins was 105 kD (*arrowhead*, Fig. 6) as expected, which enables us to distinguish them from the endogenous baculovirus kinesin (Fig. 6, lanes *e* and *f*, *upper square dots*). These proteins bound to MTs in the presence of 2 mM AMP-PNP (lanes *c* and *d*). However, when these MT pellets were extracted with 5 mM Mg-ATP, although all the other polypeptides including endogenous kinesins

(−120 kD) (*upper dots*, lanes *e* and *f*) and dynamins (−100 kD) (*lower dots*, lanes *e* and *f*) were similarly extracted from the MTs in both preparations, the 105-kD recombinant proteins were specifically extracted only in the wild-type preparation (lanes *e* and *g*) and not in the T93N-mutant preparation (lanes *f* and *h*), indicating that T93N mutant strongly binds to MTs even in the presence of Mg-ATP. To further confirm the correlation of in vivo behavior of mutant KHCs with the in vivo property, we also expressed T93S- and T93I mutants in Sf9 cells. According to the transfection study (Fig. 4, *C* and *D*), it is expected that the former binds MTs in ATP-dependent manner, and the latter binds MTs strongly even in the presence of ATP. Lanes *k* and *l* in Fig. 6 are the ATP extracts of MT pellets of the crude extracts obtained from Sf9 cells that express T93I- (lane *k*) and T93S- (lane *l*) mutant proteins, corresponding to the lanes *e* and *f*. A 105-kD T93S-mutant polypeptide was specifically eluted from the MTs in the presence of MgATP (*arrowhead*, lane *l*), while T93I mutant was not, as expected.

We also checked a motor property of this mutant by in vitro motility assay. For this purpose, we purified the wild-type and mutant recombinant 105-kD proteins from Sf9 cells. Because nucleotide-dependent MT-binding property could not be used in this mutant purification, we took advantage of specific association of polyhistidine tags to nickel column, which enabled us to purify both wild-type and mutant proteins in the same one-step procedure and separate them from the endogenous motor proteins of the insect cells. These purified proteins (lanes *i* and *j*) were used for in vitro motility assay. The T93N mutant supports MT binding to the coverslips, but never caused MT motility, although the control wild-type recombinant protein supported both MT binding and motility. Because both proteins were expressed and purified at the same time in the same procedure, these differences of motility are attributed to the point mutation of the motor domain. These in vitro properties were quite in accordance with the in vivo observation, indicating that the T93N mutant is in the strong binding state with MTs even in the presence of ATP, tempting us to call the mutant rigor type.

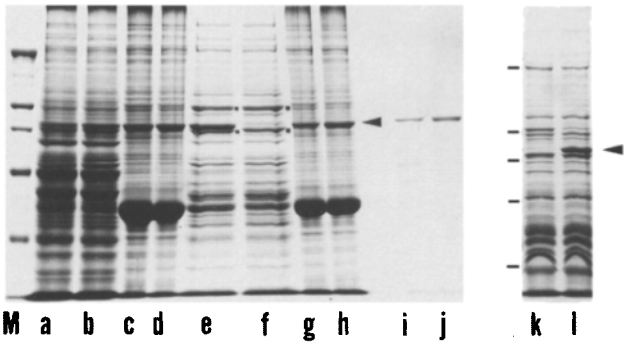

Figure 6. MT-binding property of wild-type and T93N KHC. (Lanes *a* and *b*) Crude extracts of Sf 9 cells 48 h after infection with wild-type KHC virus (lane *a*) and T93N-mutant virus (lane *b*). These extracts were incubated with taxol-polymerized MTs in the presence of 2 mM ANP-PNP and centrifuged at 100,000 *g* for 30 min. A 105-kD polypeptide is one of the major bands in MT pellets in both wild-type (lane *c*) and T93N-mutant (lane *d*) preparations. The MT pellets (lanes *c* and *d*) were incubated with 5 mM Mg-ATP and again centrifuged. The supernatants (lanes *e* and *f*) and the pellets (lanes *g* and *h*) of the wild-type KHC (lanes *e* and *g*) and T93N mutant (lanes *f* and *h*) were applied to the gels with the same amounts. (Lanes *i* and *j*) Nickel column–purified wild-type (lane *i*) and T93N (lane *j*) polypeptides. These fractions were used for in vitro motility assay. (Lanes *k* and *l*) The ATP extracts of T93I (lane *k*) and T93S (lane *l*) mutants, which corresponds to lanes *e* and *f*. *Arrowheads*, recombinant KHC polypeptides. Upper and lower dots in lanes *e* and *f* correspond to the bands for endogenous kinesin and dynamin, respectively. Lane *m* and the bars at the left of lane *k* indicate molecular mass: (from top to bottom) 200-, 116-, 97-, 66-, and 42 kD.

Stationary Localization of Membrane Organelles Is Not Affected by the Wild-type or Mutant Kinesins

Since kinesin is thought to be involved in membrane transports to the plus-end of MTs, we tested whether the overexpression of kinesin mutants causes a blockade of membrane transports in the cells. For this purpose, we focused on wild-type kinesin and T93N-mutant transfected cells,

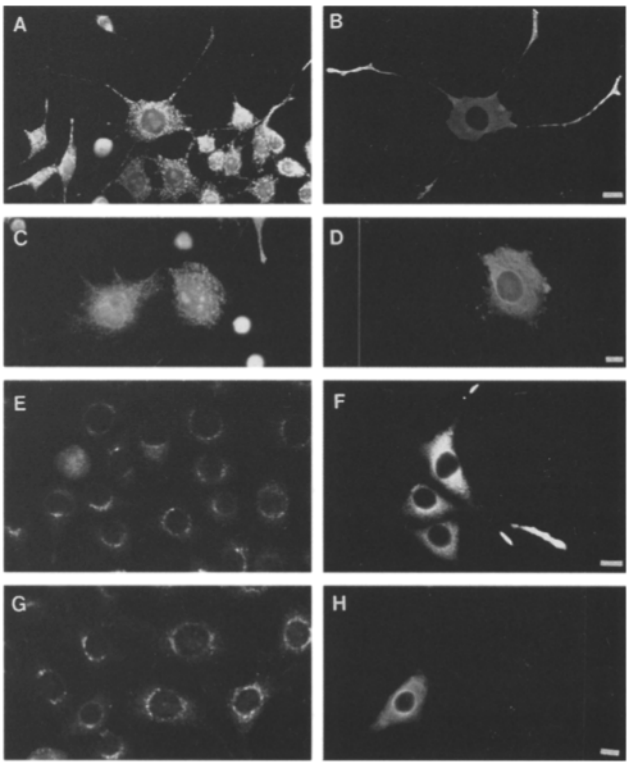

Figure 7. Localization of membrane organelles in wild-type kinesin and T93N-transfected cells. (*A–D*) Localization of mitochondria. Double labeling of wild-type kinesin-transfected cell (*A* and *B*) and T93N-transfected cell (*C* and *D*) with Mitotracker (*A* and *C*) and anti-kinesin antibody (*B* and *D*). In both transfectants, as well as in the nontransfected cells, mitochondria distribute throughout the cytoplasm and no difference is apparent between the wild-type and mutant kinesins. (*E–H*) Localization of the Golgi apparatus is not affected by the transfection of wild-type and mutant kinesins. Double labeling of wild-type kinesin-transfected cell (*E* and *F*) and T93N-transfected cell (*G* and *H*) with anti-β-COP antibody (*E* and *G*) and anti-kinesin antibody (*F* and *H*). In all cells, perinuclear accumulation of β-COP staining occurs. Bars, 20 μm.

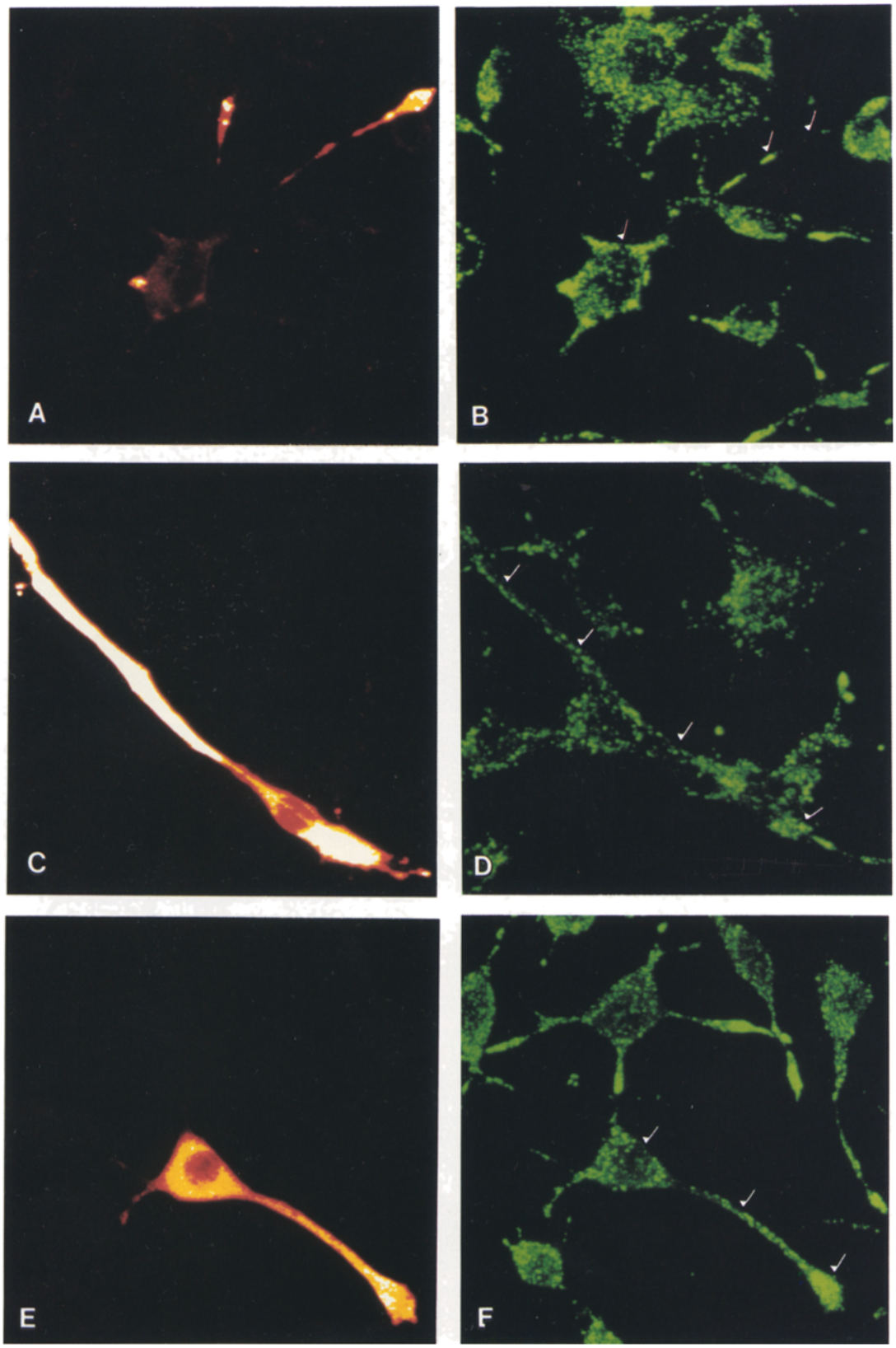

Figure 8. Anterograde lysosome movements are blocked in T93N mutant cells. Double labeling of L cells treated with NH_4Cl for 15 min (*A*, *B*, *G*, and *H*) and with NH_4Cl-Ringer's and then acetate-Ringer's for 15 min (*C–F* and *I–L*) by anti-kinesin antibody (*A*, *C*, *E*, *G*, *I*, and *K*) and anti–lamp-2 antibody (*B*, *D*, *F*, *H*, *J* and *L*). Cells indicated by arrows are transfected with wild-type KHC (*A–D*), T93S mutant (*E* and *F*), and T93N mutant (*G–L*). Note that lysosomes accumulate in the perinuclear region in most of the cells treated with NH_4Cl (*A*, *B*, *G*, and *H*). The accumulation was also observed in wild-type and T93N-transfected cells (*arrows*, *B* and *H*). In *C–F* and *I–L*,

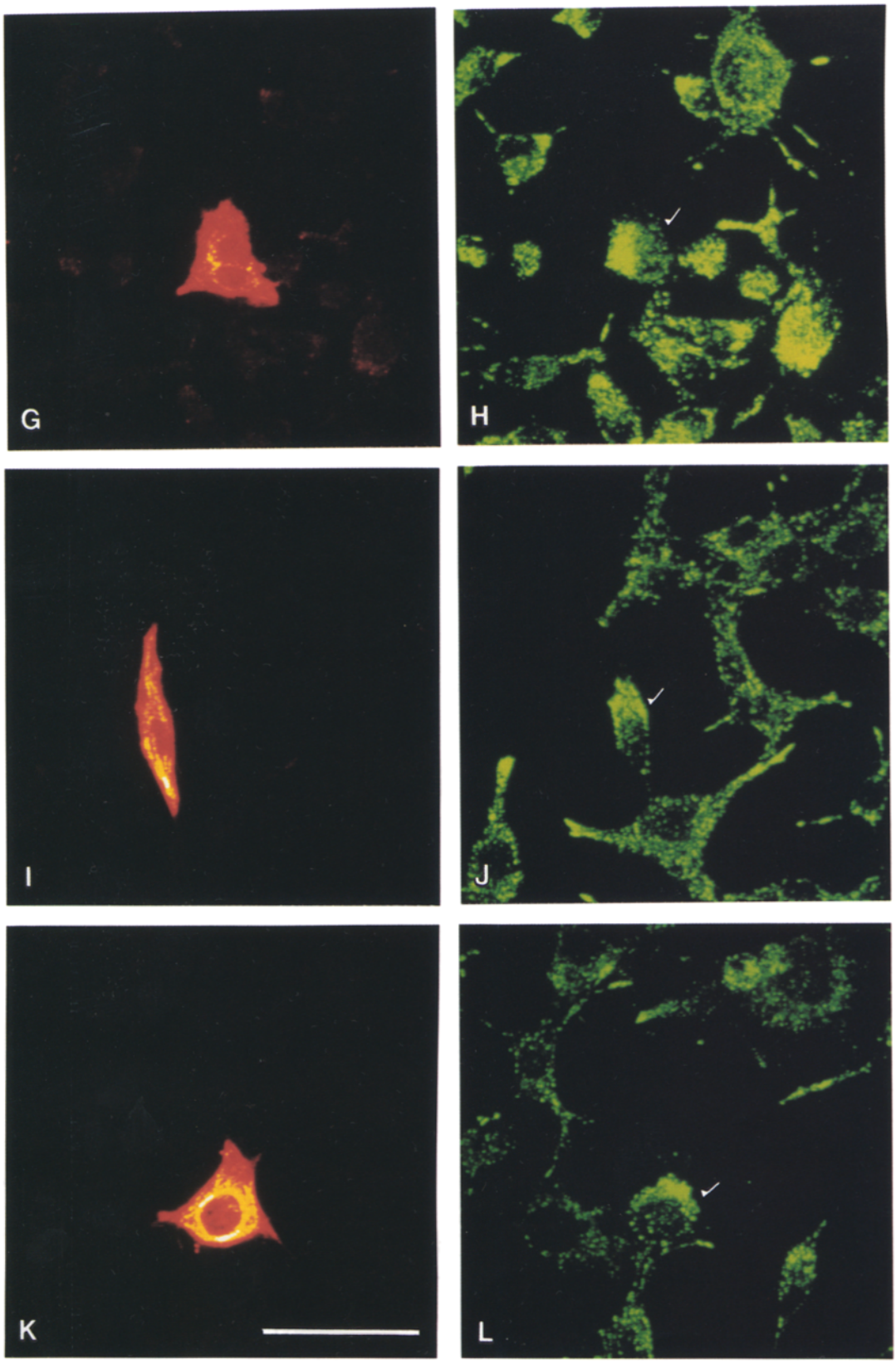

lysosomes move from the perinuclear region throughout the cytoplasm due to the rebound acidification of the cytoplasm. Lysosomes also dispersed throughout the cells transfected with wild-type KHC (*C* and *D*) and with T93S-mutant (*E* and *F*). However, lysosomes remain accumulated in T93N mutants after rebound acidification (*arrows*, *J* and *K*). Bars, 20 μm.

because preliminary experiments revealed no significant difference in membrane phenotype between the G91A/V-T93S mutants and wild-type kinesin, and between T93I- and T93N mutants.

First, using several markers, we noticed that the localizations of various kinds of membrane organelles are not severely affected by the expression of these molecules. Mitochondria, which localize and move along MTs (Ball and Singer, 1982), were stained with Mitotracker, a specific marker for this organelle (Whitaker et al., 1991). In both kinesin and the rigor-mutant transfected cells, mitochondria were widely distributed throughout the cytoplasm (Fig. 7, *A–D*), though no apparent difference exists between their localization in the wild-type kinesin, T93N-mutant transfected cells, and nontransfected cells. When we stained the Golgi apparatus with anti–β-COP antibody (M3A5) (Donaldson et al., 1990), perinuclear staining was observed in both transfectants (Fig. 7, *E–H*); thus its assembly was maintained in them. We additionally stained lysosomes, which also localize along MTs (Heuser, 1989), with anti–lamp-2 antibody, a monoclonal antibody to a lysosome membrane glycoprotein (Chen et al., 1985). In the standard buffer condition, however, considerable heterogeneity in lamp-2 localization of normal L cells prevented us to judge the influence of transfection on the lamp-2 localization: lysosomes accumulated in the cell center in some cells, and dispersed throughout the cytoplasm in the others. Thus, we decided to synchronize the lysosome localization among the cells by pharmacological treatments.

Anterograde But Not Retrograde Lysosome Membrane Transport Is Blocked by the Rigor-type Kinesin Mutants

To examine fast transports of membrane organelles, we next focused our attention on the two phenomena observed in fibroblasts related to the dynamics of membrane organelles. One is pH-dependent dispersion and centralization of lysosomes, while the other is BFA-dependent assembly and disassembly of the Golgi apparatus. Both have similar features in that: (*a*) they are MT-dependent processes, (*b*) they show rapid reversible processes occurring within 15 min, and (*c*) the localization of membranes in each extreme state is similar: the accumulation in the perinuclear region and the dispersion throughout the cytoplasm.

Lysosomes in various cell types bidirectionally move along MTs according to changes in cytoplasmic pH (Heuser, 1989). Their redistribution is reversible, in that cytoplasmic acidification accumulates them in the center of the cell, while cytoplasmic alkalinization disperses them throughout it. Using this system, we analyzed the effects of mutant kinesins on the membrane transport in L cells. As shown in Fig. 8, *B* and *H*, lysosomes accumulate in the perinuclear region within 15 min after NH_4Cl treatment. This accumulation occurs in the wild-type kinesin transfectants and also the rigor-mutant–transfected ones (Fig. 8, *A*, *B*, *G*, and *H*). In the former transfectants, similar to the normal L cells, lysosomes dispersed after 15 min when the cells were treated with acetate buffer (Fig. 8, *C* and *D*). In the latter transfectants, however, they instead remained in the perinuclear regions (Fig. 8, *I–L*).

After the cells were initially treated with NH_4Cl buffer

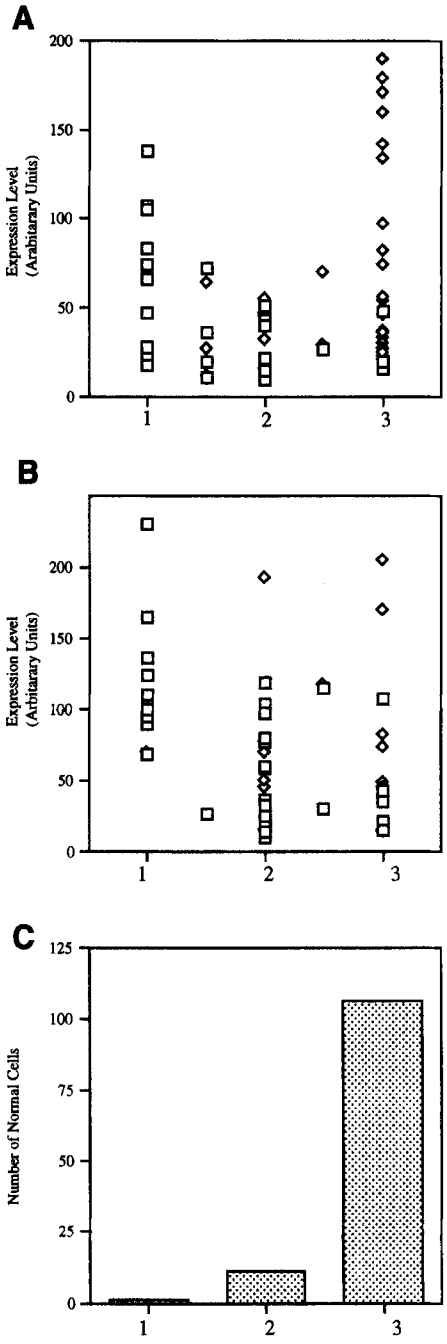

Figure 9. Quantitative analysis of the lysosome distribution of wild-type and rigor-mutant kinesin-transfected cells after NH_4Cl followed by acetate treatment. The accumulation of lysosomes after NH_4Cl then acetate treatment was plotted against the expression level of KHC. The protein expression level was quantified as shown in Fig. 3. The distribution of lysosomes were single blindedly classified into (*1*) accumulation around cell center; (*2*) accumulation around cell center and loose cytoplasmic staining; and (*3*) dispersion throughout cytoplasm (Heuser, 1989). The classification was independently performed twice, and each cell was finally classified according to the average of the scores. *A* and *B* show the results of independent two sets of experiments. *C* shows the control distribution of the nontransfected L-cell population. Rigor-mutant, but not wild-type KHC blocks dispersion of lysosomes after NH_4Cl then acetate treatment. *Square*, each T93N-mutant cell; *diamond*, wild-type KHC cell.

and then acetate buffer, the rebound effect potentiated lysosome dispersion in >80% of the nontransfected L cells. In contrast, lysosomes were tightly clustered at the cell center in the cells transfected with the T93N mutant, presumably because pretreatment with NH_4Cl accumulates lysosomes at the cell center, but the subsequent dispersion step was blocked. Hence, in this treatment, the use of lamp-2 staining enables us to distinguish T93N-mutant transfectants from the many nontransfected cells (Fig. 8, *J* and *L*). In contrast, lysosomes localize diffusely in the cytoplasm or in the processes of nontransfected cells (Fig. 8, *C* and *D*). The same tendency was observed in the T93I mutant (data not shown). This result is important because it clearly shows that only anterograde movement of lysosomes is blocked by the rigor-mutant transfection.

The results were quantitatively shown in Fig. 9. The results of two typical independent batches of experiments are shown in Figs. 9, *A* and *B*. These figures show that higher expression of the T93N mutant blocks the dispersion of lysosomes, while the expression of the wild-type kinesin does not.

In the previous study (Heuser, 1989), it was shown that lysosomes disperse when MTs are depolymerized. Thus it was unclear whether MTs are functional when the lysosomes disperse after acidification. However, the lack of this effect upon acidification of the T93N-mutant transfectants strengthens the argument that MTs are functional for the anterograde transport of lysosomes.

Bidirectional Vesicular Transport between the Golgi Apparatus and ER Was Not Blocked by the Wild-type or Mutant Kinesins

In both wild-type and rigor-mutant–transfected cells, the BFA treatment disassembled the Golgi apparatus, and within 15 min after washout of BFA, it reassembled in the perinuclear region (Fig. 10). This similarity is in clear contrast to the difference found with respect to pH-dependent lysosome dispersion (Fig. 8).

Because β-COP dissociates from the Golgi apparatus soon after BFA treatment (Donaldson et al., 1990), it is possible that the Golgi apparatus does not actually reassemble in rigor-mutant cells, although the dissociation and reassociation of β-COP with the Golgi apparatus still occurs. To exclude this possibility, we used BODIPY-ceramide, another marker for the Golgi apparatus (Pagano et al., 1991). With this marker, resultant strong staining of the perinuclear region (Fig. 11 *A*) should vanish within 15 min after treatment with BFA (Fig. 11, *D* and *G*). Although BODIPY-ceramide can stain living cells, it cannot stain permeabilized cells; thus it is impossible to directly double label with anti-kinesin antibody. To mitigate this drawback, we cotransfected rigor-type mutant cDNA with CD8 cDNA. Because CD8 is expressed on the cell surface, it can be stained by immunocytochemistry without permeabilization. The living cells were first stained by BODIPY-ceramide and anti-CD8 antibody, and then photographed. After this, they were permeabilized and stained with anti-kinesin antibodies. Results showed that the CD8 expression on the cell surface is not affected by the expression of the wild-type KHC or T93N mutant (Fig. 11, *C* and *F*), which is consistent with the fact that constitutive secretion is MT independent (Rivas and Moore, 1989). The cells expressing both CD8 (Fig. 11 *C*) and the T93N mutant (Fig. 11 *F*) showed diffuse BODIPY-ceramide staining after the BFA treatment (Fig. 11, *D* and *G*, *arrowheads*). This confirms that disassembly of the Golgi apparatus also occurs in the rigor-mutant cells.

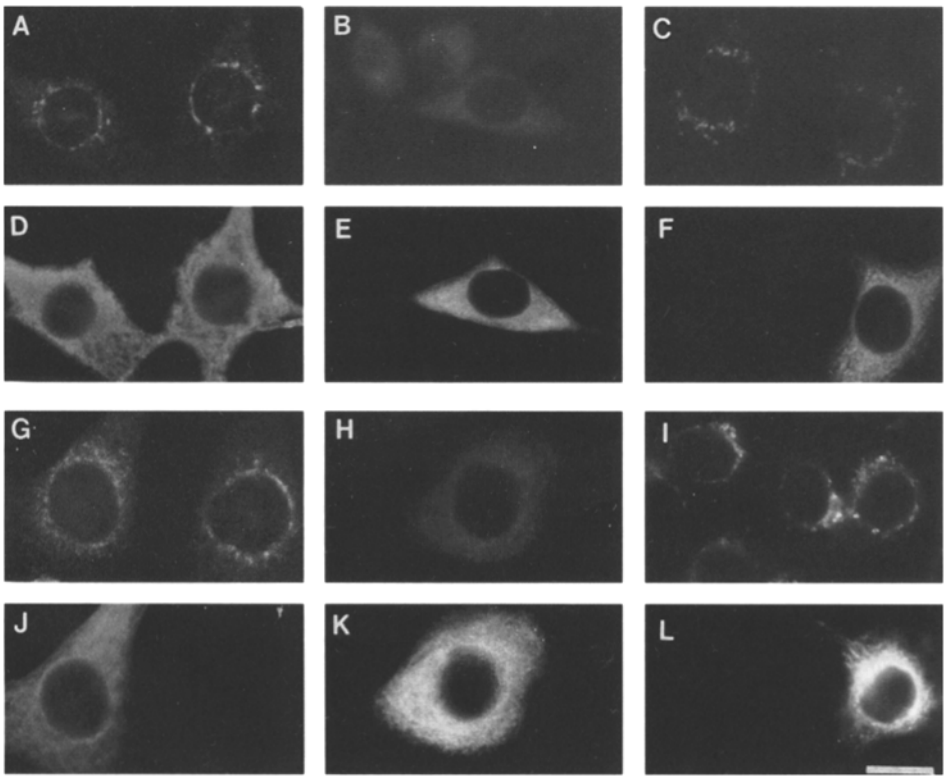

Figure 10. BFA-dependent disassembly and reassembly of Golgi apparatus in wild-type and T93N-mutant kinesin-transfected cells. 48 h after transfection, L cells (*A*, *D*, *G*, and *J*) were incubated with 5 μg/ml BFA for 15 min (*B*, *E*, *H*, and *K*), then washed with medium twice and incubated for another 15 min (*C*, *F*, *I*, and *L*). (*A–F*) Double labeling of wild-type kinesin-transfected cells with anti–β-COP antibody (*A–C*), and anti-kinesin antibody (*D–F*). (*G–L*) Double labeling of T93N-mutant–transfected cells with anti–β-COP antibody (*G–I*), and anti-kinesin antibody (*J–L*). In both cases, disassembly and rapid recovery of Golgi apparatus is apparent. Bar, 20 μm.

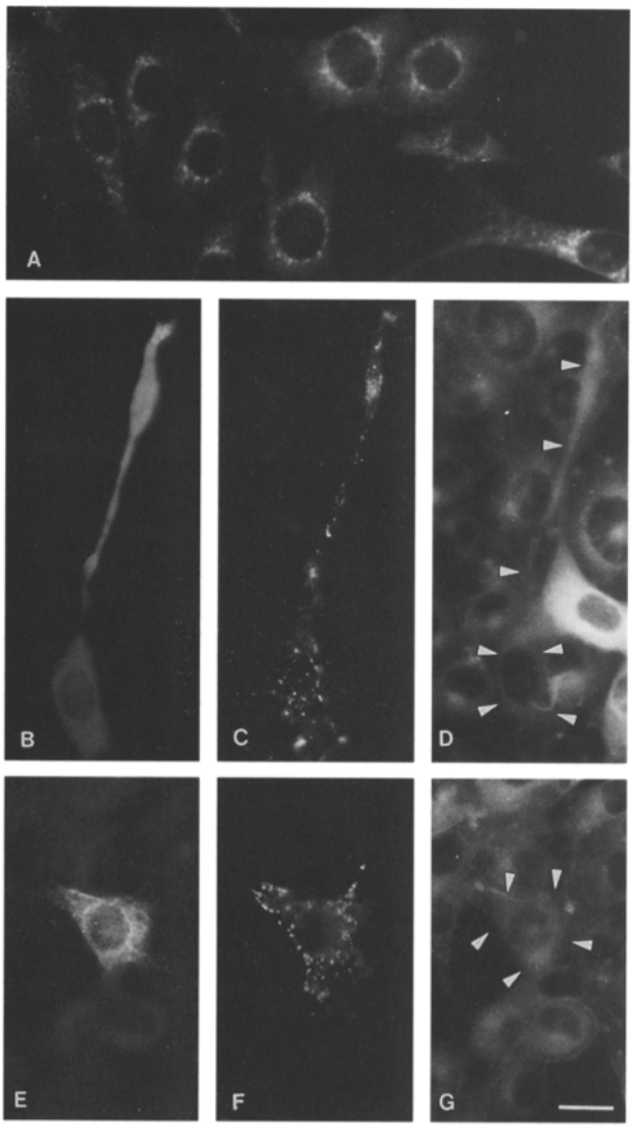

Figure 11. BFA-dependent Golgi apparatus disassembly in wild-type and T93N-mutant transfectants. BODIPY-ceramide stains the perinuclear region of L cells (*A*). The 15-min treatment with BFA completely disrupts the staining by BODIPY-ceramide (*D* and *G*). The cells marked by arrowheads are wild-type and T93N-mutant–transfected cells (*D* and *G*, respectively). To detect these cells, we performed cotransfection with kinesin and CD8 cDNAs. CD8 was expressed on the plasma membrane, and the living cell was stained by adding antibodies to the medium. The living cells were first photographed after BODIPY-ceramide staining (*D* and *G*) and CD8 staining (*C* and *F*) then fixed with ice-cold methanol, stained with anti-kinesin antibody, and photographed for kinesin staining (*B* and *E*) and CD8 staining (*C* and *F*). Bar, 20 μm.

Discussion

In this paper, we established a point mutation that makes kinesin always in a strong binding state with MTs in vitro. Second, we showed the simple transfection assay is effective to screen the mutants of motor protein activity. Third, we found that the overexpression of wild-type KHC promotes the elongation of the cellular processes of L cells. Finally, we showed that the rigor-type mutant expression causes a selective, dominant phenotype on an anterograde vesicular transport.

T93N- and T93I-Mutant Kinesins Strongly Bind MTs In Vitro and In Vivo

T93N- and T93I mutants tightly bind to MTs in vivo and in vitro. Wild-type kinesin is in a strong binding state with MTs when it is in the ADP form, and in a weak binding state when it is in the ATP form (Hackney, 1988). In contrast, T93N- and T93I mutants are in a strong binding state even in the presence of ATP. Although nod, a kinesin-like motor protein in the fruit fly, has a corresponding mutant of dominant phenotype (Rasooly et al., 1991), it is not known whether the mutant nod binds strongly MTs. In the case of GTP-binding proteins, the corresponding mutations of S/T in the nucleotide-binding motif are reported in *ras* p21 (S17N) or α subunit of G-protein (S54N), and showed preferential affinities to GDP (Farnsworth and Feig, 1991; Hildebrandt et al., 1991). Thus T93N and T93I are the first mutants that are biochemically shown to change motor activity in vitro.

Localization of Wild-type and Mutant Kinesins in the Cells

The localization of wild-type and mutant kinesins in transfected cells well reflected their motor domain properties in vitro. T93N- and T93I mutants were shown to be in a strong binding state with MTs in vitro (Fig. 6). This property was just like the ones expected from the in vivo localization of the mutants (Fig. 5). The mutant proteins localized on the MTs even after detergent extraction in the presence of ATP. It did not promote process elongation (Fig. 4). In contrast, wild-type KHC binds to MTs in ATP-dependent manner and translocates on MTs in vitro (Fig. 6). In transfected cells, it was accumulated at the tips of the processes, which are the plus-end terminal of MT rails, and was washed away by the same detergent extraction even in the absence of ATP (Fig. 5). T93S mutant is substituted T93 to S, just like T93I and T93N mutants, but still conserves the ATP-binding motif whose last amino acid is either Thr or Ser. This mutant showed a property just like wild-type KHC both in vivo and in vitro. Thus, simple transfection was a sensitive assay to screen the mutant kinesins whose motor functions are genetically altered. In fact, transfection of a mutant whose putative MT-binding motifs was altered (E337Q in DLAGSE consensus motif for kinesin superfamily proteins) showed no binding with MTs and no accumulation at the cell periphery (data not shown).

Transient expression of the human KHC in CV1 cells produced both a diffuse distribution and a filamentous staining pattern that coaligns with MTs (Navone et al., 1992). However, we did not observe any filamentous pattern in the mouse wild-type KHC-transfected cells. The apparent discrepancy may be due to a slight difference in the cytoplasmic ATP concentration of the transfected cells. Kinesin binds MTs efficiently only after the addition of AMP-PNP or the depletion of ATP in vitro (Vale et al., 1985). We presume that kinesin bound to MTs in the CV1 cells because of the consumption of ATP by the overexpressed motor protein, while the ATP level was not de-

creased so much in the case of L cells that overexpressed wild-type KHC. We should note that T93N mutant binds to MTs irrespective of cellular ATP level, because it still binds to MTs even in the presence of 5 mM ATP after saponin extraction.

The localization of overexpressed wild-type KHC raised a question: why doesn't native kinesin appear to accumulate at the plus-end terminal of MT array in cells? For example, kinesin localize in the mitotic spindle in sea urchin eggs while the plus-end of MTs is in the cell periphery (Heason et al., 1992). Polarity of MTs in neuronal axons are the plus-ends to the axon terminal. Nevertheless, kinesin does not accumulate at the growth cones or synaptic terminals (Hollenbeck, 1989; Pfister et al., 1989; Niclas et al., 1994). This simple consideration leads us to the idea that the localization of native kinesin is not motor dependent, but well-regulated by other factors. The overexpressed KHC must be somehow out of this regulation in the cells. One possible mechanism is that the degradation or retrograde transport of kinesin occurs in the cell periphery. The former is suggested by our previous study of the immunocytochemistry of kinesin in ligated axons (Hirokawa et al., 1991). The overexpression of KHC may prevail this process and then KHC accumulates at the tips. The other mechanism is that the motility of native kinesin molecules is suppressed until it becomes necessary. Kinesin light chains decrease the ATPase activity of KHCs when they are in cytosolic form (Hackney et al., 1991). The cytosolic pool of kinesin tetramer may then be in the off state, and does not traverse along the MTs in normal cells. However, most of the overexpressed KHCs may lack their light chains, and therefore, they are always in the on state even when they are not associated with their cargoes, and move along MTs to the tips of the cells.

The fact that the localization of overexpressed KHC tells us much about the motor activity gave us the idea that it does not tell us much about the cargoes. A number of immunolocalization studies of endogenous kinesin were performed (Hollenbeck, 1989; Pfister et al., 1989; Hirokawa et al., 1991; Heason et al., 1992; Marks et al., 1994; Niclas et al., 1994; Lippincott-Schwartz et al., 1995), but there are still arguments on the cargoes of kinesin. This is presumably due to the fact that only one or a few kinesin molecules are actually responsible for a given motion of vesicles (Howard et al., 1989), although lots of kinesin exists around the organelles as soluble, weakly membrane bound, and tightly membrane bound forms, and accordingly, the amount of kinesin associated with certain vesicles cannot always be a crucial clue to the identification of the cargoes. Thus we took a strategy to compare the phenotypes of the wild-type and the mutant-transfected cells, expecting that the overexpression of these proteins may interfere with the function of endogenous kinesin. Exogenous kinesin is expressed so much (Fig. 1) in transfected cells that the majority of the kinesin (both endogenous and exogenous kinesin) cannnot bind to the cargoes and exists in the cytoplasmic pool, while the majority of the cargoes are saturated with exogenous kinesin via competition with endogenous kinesin. For these reasons, we used the antikinesin staining only as a marker for the transfected cells and an indicator of its expression level in the study of cellular function of kinesin (Figs. 7–11).

Overexpressed KHC Promoted the Process Elongation

L cells expressing exogenous wild-type KHC had significantly longer processes than the nontransfected cells. Mouse L cells originally have a tendency to protrude thin processes from the cell bodies up to 50 μm in length, but the processes of the KHC overexpressed cells were often as long as 100 μm (Fig. 3). On the other hand, the number of the processes was not increased significantly. The transfection of the KHC to the cells that do not have processes (3T3 cells or CHO cells) scarcely made such a process formation (data not shown). T93N mutant did not promote process elongation.

The mechanism for this process elongation should be different from that which occurs in the cells into which cDNAs of MAPs (microtubule-associated proteins) are introduced (Kanai et al., 1989). First, these processes are thinner and longer than the MAPs-induced processes. Second, bundling of MTs was not observed in these cells as observed in the MAP-transfected cells. Third, wild-type KHC is not tightly associated with MTs, while MT binding and bundling are believed to be the mechanisms of the process formation of the MAPs overexpressing cells. Antisense study showed that the inhibition of the KHC expression does not inhibit process initiation of neurons, but suppressed the elongation of the processes (Ferreira et al., 1992), suggesting that KHC is involved in the process elongation by transporting the plasma membrane precursors to the growth cone, where it is believed to be a site for a new plasma membrane insertion (Pfenninger and Mayle-Pfenninger, 1981). Thus the present process elongation may be due to the enhanced sorting of plasma membrane precursor vesicles along the processes. If so, the new surface membrane preferentially was added at the tips of processes, which in turn would elongate the processes. When the plasma membrane and its precursor meet at growth cones, they will fuse together immediately and kinesin would dissociate from the membrane. In fact, kinesin is not reported to accumulate on the vesicles in growth cones. This would also be the case in this overexpression system, because overexpressed kinesin was easily extracted after saponin permeabilization (Fig. 2 *F*).

Rigor-type Kinesins Show a Dominant Phenotype in Membrane Transport

In the rigor-type mutant-transfected cells, we found the stationary localization of mitochondria, the Golgi apparatus, and lysosomes to be similar to that occurring in control cells (Figs. 7 and 8). The rapid redistribution of the Golgi apparatus was not affected (Fig. 10 and 11), nor was the accumulation of lysosomes at the cell center (Fig. 8, *G* and *H*), though their dispersion to the periphery was selectively blocked (Fig. 8, *J* and *L*). When we consider the polarity of MTs in L cells, dispersion of the organelles to the periphery is MT plus-end–directed motility, and accumulation to the center is minus-end directed. Thus, the MT minus-end–directed motions were not inhibited. Between the two plus-end–directed, MT-dependent motions examined here, only one movement was blocked, which suggests that the underlying mechanisms for these two plus-end–directed vesicular transports are different.

Two possibilities were entertained that explain why the

membrane transport was blocked by the T93N- and T93I mutants. One is that the binding of the mutants to MTs inhibits the movement of organelles by a simple mechanical block, i.e., motor proteins responsible for plus-end–directed lysosome movement along MTs are competitively inhibited by the excess mutants bound to MTs. Under this interpretation, however, it is difficult to explain the selectiveness of the blockade, since a mechanical block of MTs similarly blocks the kinesin- and dynein-mediated motility in vitro (Hagiwara et al., 1994). To date, all the identified plus-end–directed MT motors for organelle transports are kinesin superfamily proteins, all of which have similar head domain structure (Pesavento et al., 1994; Kondo et al., 1994; Sekine et al., 1994; Nangaku et al., 1994; Noda et al., 1995; Okada et al., 1995; Yamazaki et al., 1995). Thus, all the plus-end–directed motility should be similarly blocked by this head competition mechanism, which is inconsistent with the present result that MT plus-end–directed (retrograde) transport from the Golgi apparatus to the ER was not blocked.

The other possibility concerns the association between the mutant proteins and cargoes, i.e., most of the cargoes will competitively bind to the mutant KHCs, which in turn bind tightly to MTs in the center of the cells. The tail domain of KHC was shown to be necessary and sufficient for the membrane binding in vitro (Skoufias et al., 1994). Under this interpretation, lysosomes are one of kinesin's cargoes, whereas plus-end–directed transport vesicles moving from the Golgi apparatus to the ER are not. This is supported by the observations that the transport of lysosome in macrophage was inhibited by a monoclonal antibody specific for kinesin (Hollenbeck and Swanson, 1990), and that lysosome but not Golgi apparatus dispersion is inhibited by the antisense oligonucleotide treatment in cultured neurons or glial cells (Feiguin et. al., 1994). Recently, it has been reported that injection of H1 antibody blocks Golgi apparatus to ER movement (Lippincott-Schwartz et al., 1995), but the injected antibody has not been shown to block motility in vitro and they did not see the effect of antibody injection to lysosomal movements, thus it is not determined yet which movements (lysosome or Golgi apparatus to ER) is more liable to the perturbation.

To obtain the MT minus-end–directed motility, the lysosomes may detach from the plus-end–directed motor (mutants), and be transported by a minus-end–directed motor such as dynein. Although it is not known what kind of motors mediate plus-end–directed (retrograde) movement from the ER to the Golgi apparatus, there is an accumulation of evidences indicating the existence of a number of MT plus-end–directed motors for vesicular transports, which suggests that each motor may play some specific role in vesicular transports (Otsuka et al., 1991; Gho et al., 1992; Hirokawa, 1993).

The dominant phenotype of rigor-kinesin mutants presented here dissected membrane transports in L cells. Previous approaches such as nocodazole or BFA treatments have shown multiple effects on cellular membrane trafficking, hence making it difficult to analyze the direct effect of these perturbations. Since the rigor mutants constructed here produce a more specified effect on membrane transport, they provide a unique model system for analyzing of membrane events in detail, e.g., constitutive/regulated secretions and transcytosis. For these purposes, polarized cells such as epithelial cells and neurons are most suitable, since the plasma membrane and cell center in fibloblasts are so close that MT-dependent transport may not be essential for these processes. On the other hand, especially in neurons, the cargoes must inevitably be transported along long axons or dendrites via a MT-dependent process. In addition, because neurons contain well-characterized membrane marker proteins such as synaptic vesicle proteins, they are advantageous to identify various different kinds of membrane organelles. Further research is currently underway using these approaches to elucidate mechanisms involved in neuronal membrane transports.

We thank Dr. Nancita R. Lomax (National Cancer Institute) for providing taxol, Dr. G. S. Bloom for the H1 and H2 antibodies, Dr. K. Kato for cDNAs, and Dr. T. E. Kreis for M3A5 antibody.

This work was supported by a special grant-in-aid to N. Hirokawa for scientific research from the Ministry of Education, Science and Culture of Japan.

Received for publication 14 March 1995 and in revised form 11 July 1995.

References

Ball, E. H., and S. J. Singer. 1982. Mitochondria are associated with microtubules and not with intermediate filaments in cultured fibroblasts. *Proc. Natl. Acad. Sci. USA.* 79:123–126.

Brady, S. T. 1985. A novel brain ATPase with properties expected for the fast axonal transport motor. *Nature (Lond.).* 317:73–75.

Chen, J. W., T. L. Murphy, M. C. Willingham, I. Pastan, and J. T. August. 1985. Identification of two lysosomal membrane glycoproteins. *J. Cell Biol.* 101: 85–95.

Chen, C., and H. Okayama. 1987. High-efficiency transformation of mammalian cells by plasmid DNA. *Mol. Cell. Biol.* 7:2745–2752.

Donaldson, J. G., J. Lipincott-Schwartz, G. S. Bloom, T. E. Kreis, and R. D. Klausner. 1990. Dissociation of a 110-kD peripheral membrane protein from the Golgi apparatus is an early event in brefeldin A action. *J. Cell Biol.* 111: 2295–2306.

Farnsworth, C., and L. A. Feig. 1991. Dominant inhibitory Ha-ras mutations in the Mg^{2+} binding site of ras blocks its activation by GTP. *Mol. Cell. Biol.* 11: 4822–4829.

Feiguin, F., A. Ferreira, K. S. Kosik, and A. Caceras. 1994. Kinesin-mediated organelle translocation revealed by specific cellular manipulation. *J. Cell Biol.* 127:1021–1039.

Ferreira, A., J. Niclas, R. D. Vale, G. A. Banker, and K. S. Kosik. 1992. Supression of kinesin expression in cultured hippocampal neurons using antisense oligonucleotides. *J. Cell Biol.* 117:595–606.

Gho, M., K. McDonald, B. Ganetzky, and W. M. Saxton. 1992. Effects of kinesin mutations on neuronal functions. *Science (Wash. DC)* 258:313–316.

Goldstein, L. S. B. 1991. The kinesin superfamily:tails of redundancy. *Trends Cell Biol.* 1:93–98.

Hackney, D. D. 1988. Kinesin ATPase: rate-limiting ADP release. *Proc. Natl. Acad. Sci. USA.* 85:6314–6318.

Hackney, D. D., J. D. Levitt, and D. W. Wagner. 1991. Characterization of $a_2\beta_2$ and a_2 forms of kinesin. *Biochem. Biophys. Res. Comm.* 174:810–815.

Hagiwara, H., H. Yorifuji, R. Sato-Yoshitake, and N. Hirokawa. 1994. Competition between motor molecules (kinesin and cytoplasmic dynein) and fibrous microtubule-associated proteins in binding to microtubules. *J. Biol. Chem.* 269:3581–3589.

Heason, J. H., D. Nebitt, B. D. Wright, and J. M. Scholey. 1992. Immunolocalization of kinesin in sea urchin coelomocytes. Association of kinesin with intracellular organelles. *J. Cell. Sci.* 103:309–320.

Heuser, J. 1989. Changes in lysosome shape and distribution correlated with changes in cytoplasmic pH. *J. Cell. Biol.* 108:855–864.

Hildebrandt, J., R. Day, C. L. Farnsworth, and L. A. Feig. 1991. A mutation in the putative Mg^{2+} binding site of G_{sa} prevents its activation by receptors. *Mol. Cell. Biol.* 11:4830–4838.

Hirokawa, N. 1982. The crosslinker system between neurofilaments, microtubules, and membranous organelles in frog axons revealed by quick-freeze, deep-etching method. *J. Cell. Biol.* 94:129–142.

Hirokawa, N., R. Sato-Yositake, N. Kobayashi, K. K. Pfister, G. S. Bloom, and S. T. Brady. 1991. Kinesin associates with anterogradely transported membranous organelles in vivo. *J. Cell Biol.* 114:295–302.

Hirokawa, N. 1993. Axonal transport and the cytoskeleton. *Curr. Opin. Neurobiol.* 3:724–731.

Hollenbeck, P. J., and J. A. Swanson. 1990. Radial extension of macrophage tubular lysosomes supported by kinesin. *Nature (Lond.).* 346:864–866.

Hollenbeck, P. J. 1989. The distribution, abundance, and subcellular localiza-

tion of kinesin. *J. Cell Biol.* 108:2335–2342.
Howard, J. A., J. Hudspeth, and R. D. Vale. 1989. Movement of microtubules by single kinesin molecules. *Nature (Lond.).* 342:154–158.
Kanai, Y., R. Takemura, T. Ohshima, H. Mori, Y. Ihara, M. Yanagisawa, T. Masaki, and N. Hirokawa. 1989. Expression of multiple tau isoforms and microtubule bundle formation in fibroblasts transfected with a single tau cDNA. *J. Cell Biol.* 109:1173–1184.
Kato, K. 1991. Sequential analysis of twenty mouse brain cDNA clones selected by specific expression patterns. *Eur. J. Neurosci.* 2:704–711.
Kondo, S., R. Sato-Yoshitake, Y. Noda, H. Aizawa, T. Nakata, Y. Matumura, and N. Hirokawa. 1994. KIF3A is a new microtubules based anterograde motor in the nerve axons. *J. Cell Biol.* 125:1095–1107.
Lippincott-Schwartz, J., J. G. Donaldson, A. Schweizer, E. G. Berger, H.-P. Hauri, L. C. Yuan, and R. D. Klausner. 1990. Microtubule dependent retrograde transport of proteins into the ER in the presence of brefeldin A suggests an ER recycling pathway. *Cell.* 60:821–836.
Lippincott-Schwartz, J., N. B. Cole, A. Marotta, P. A. Conrad, and G. S. Bloom. 1995. Kinesin is the motor for microtubule-mediated Golgi-to-ER membrane traffic. *J. Cell Biol.* 128:293–306.
Lye, R. J., M. E. Porter, J. M. Scholey, and J. R. McIntosh. 1987. Identification of a microtubule-based cytoplasmic motor in the nematode *C. elegans*. *Cell.* 51:309–318.
Marks, D. L., J. M. Larkin, and M. A. McNieven. 1994. Association of kinesin with the Golgi apparatus in rat hepatocytes. *J. Cell Sci.* 107:2417–2426.
Meluh, P., and M. D. Rose. 1990. KAR3, a kinesin-related gene required for yeast nuclear fusion. *Cell.* 60:1029–1041.
Nakata, T., and N. Hirokawa. 1992. Organization of cortical cytoskeleton of cultured chromaffin cells and involvement in secretion as revealed by quick-freeze, deep-etching, and double-label immunoelectron microscopy. *J. Neurosci.* 12:2186–2197.
Nakata, T., R. Sato-Yoshitake, Y. Okada, Y. Noda, and N. Hirokawa. 1993. Thermal drift is enough to drive a single microtubule along its axis even in the absence of motor proteins. *Biophys. J.* 65:2504–2510.
Nangaku, M., R. Sato-Yoshitake, Y. Okada, Y. Noda, R. Takemura, H. Yamazaki, and N. Hirokawa. 1994. KIF1B: a new microtubule plus-end directed monomeric motor for mitochondria transport. *Cell.* 39:1209–1220.
Navone, F., J. Niclas, N. Hom-Booher, L. Sparks, H. D. Bernstein, G. McCaffrey, and R. D. Vale. 1992. Cloning and expression of a human kinesin heavy chain gene: interaction of the COOH-terminal domain with cytoplasmic microtubules in transfected CV-1 cells. *J. Cell Biol.* 117:1263–1275.
Niclas, J., F. Navone, N. Hom-Booher, and R. D. Vale. 1994. Cloning and localization of a conventional kinesin motor expressed exclusively in neurons. *Neuron.* 12:1059–1072.
Noda, Y., T. Nakata, and N. Hirokawa. 1993. Localization of dynamin: widespread distribution in mature neurons and association with membranous organelles. *Neuroscience* 55:113–127.
Noda, Y., R. Sato-Yoshotake, S. Kondo, M. Nangaku, and N. Hirokawa. 1995. KIF2 is a new anterograde microtubule based motor which transports membranous organelles distinct from those carried by KHC or KIF3A/B. *J. Cell Biol.* 129:157–167.
Okada, Y., H. Yamazaki, Y. Sekine, and N. Hirokawa. 1995. The neuron specific kinesin superfamily protein KIF1A is a unique monomeric motor for the anterograde axonal transport of synaptic vesicle precursors. *Cell.* 81:769–780.
Otsuka, A. J., A. Jeyaprakash, J. Garcia-Anoveros, L. Z. Tang, G. Fisk, T. Hartshorne, R. Franco, and T. Born. 1991. The *C. elegans* unc104 gene encodes a putative kinesin heavy chain-like protein. *Neuron.* 6:113–122.
Pagano, R. E., O. C. Martin, H. C. Kang, and R. P. Haugland. 1991. A novel fluorescent ceramide analogue for studying membrane traffic in animal cells: accumulation at the Golgi apparatus results in altered spectral properties of the sphingolipid precursor. *J. Cell Biol.* 113:1267–1279.
Paschal, B. M., and R. B. Vallee. 1987. Retrograde transport by the microtubule associated protein MAP1C. *Nature (Lond.).* 330:181–183.
Pesavento, P. A., R. J. Stewart, and L. S. Goldstein. 1994. Characterization of the KLP68D kinesin-like protein in Drosophila: possible roles in axonal transport. *J. Cell Biol.* 127:1041–1048.
Pfenninger, K. H., and M. F. Mayle-Pfenninger. 1981. Lectin labeling of sprouting neurons. II. Relative movement and appearance of glycoconjugates during plasmalemmal expansion. *J. Cell Biol.* 89:547–559.
Pfister, K. K., M. C. Wagner, D. L. Stenoien, S. T. Brady, and G. S. Bloom. 1989. Monoclonal antibodies to kinesin heavy and light chains stain vesicle-like structures, but not microtubules, in cultured cells. *J. Cell Biol.* 108:1453–1464.
Rasooly, R. S., C. M. New, and P. Zhang. 1991. The lethal (1) TW-6CS mutation of *Drosophila melanogaster* is a dominant antimorphic allele of nod and is associated with a single base change in the putative ATP-binding domain. *Genetics.* 129:409–422.
Rivas, R. J., and H.-P. H. Moore. 1989. Spatial segregation of the regulated and constitutive secretory pathways. *J. Cell. Biol.* 109:51–60.
Sekine, Y., Y. Okada, Y. Noda, S. Kondo, H. Aizawa, R. Takemura, and N. Hirokawa. 1994. A novel microtubule-based motor protein (KIF4) for organelle transports whose expression is regulated developmentally. *J. Cell Biol.* 127:187–202.
Skoufias, D. A., D. G. Cole, K. P. Wedaman, J. M. Scoley. 1994. The carboxyl-terminal domain of kinesin heavy chain is important for membrane binding. *J. Biol. Chem.* 29:1477–1485.
Turner, J. R., and A. M. Tartakoff. 1989. The response of the Golgi complex to microtubule alterations: the roles of metabolic energy and membrane traffic in Golgi complex organization. *J. Cell Biol.* 109:2081–2088.
Vale, R. D., T. S. Reese, and M. P. Sheetz. 1985. Identification of a novel force-generating protein, kinesin, involved in microtubule-based motility. *Cell.* 42: 39–50.
Whitaker, J. E., P. L. Moore, R. P. Haugland, and R. P. Haugland. 1991. Dihydrotetramethylrosamine: a long wavelength, fluorogenic peroxidase substrate evaluated in vitro and in a model phagocyte. *Biochem. Biophys. Res. Comm.* 175:387–393.
Yamazaki, H., T. Nakata, Y. Okada, and N. Hirokawa. 1995. KIF3A/B: a new heterodimer that works as microtubule-plus-end directed motor for fast axonal transport. *J. Cell Biol.* 130:1387–1400.
Yang, J. T., R. A. Laymon, and L. S. B. Goldstein. 1989. A three-domain structure of kinesin heavy chain revealed by DNA sequence and microtubule binding analyses. *Cell.* 56:879–889.